Available online at www.sciencedirect.com
SCIENCE DIRECT®
Biomaterials 27 (2006) 1175–1186
Biomaterials
www.elsevier.com/locate/biomaterials

Spatial control of protein within biomimetically nucleated mineral

Linh N. Luong[a], Sun Ig Hong[b], Rusha J. Patel[c], Mark E. Outslay[a], David H. Kohn[a,d,*]

[a]*Biomedical Engineering, University of Michigan, Ann Arbor, MI 48109, USA*
[b]*Metallurgical Engineering, Chungnam National University, Taejon, 305-764, Korea*
[c]*Mechanical Engineering, University of Michigan, Ann Arbor, MI 48109, USA*
[d]*Biologic & Materials Sciences, University of Michigan, Ann Arbor, MI 48109, USA*

Received 27 April 2005; accepted 25 July 2005
Available online 31 August 2005

Abstract

An ideal approach for bone tissue engineering allows for osteoconductivity, osteoinductivity, and cell transplantation. In this study, we examined coprecipitation and surface adsorption schemes with respect to their abilities to control the spatial quantity and localization of a model protein, bovine serum albumin (BSA), that is incorporated into a biomimetic apatite layer nucleated onto polylactic-*co*-glycolic acid (PLGA) films. Protein incorporation was characterized by determining protein: presence, quantity loaded, retention, effects on mineral morphology, and localization. FT-IR confirmed the presence of protein in all coprecipitation samples with stronger peaks in the coprecipitated samples compared to the surface adsorbed samples. Coprecipitation resulted in higher loading capacities and higher protein retention versus adsorption. Protein incorporation via coprecipitation changed the mineral morphology from sharp plate-like structures to more rounded structures, whereas, surface adsorption did not change mineral structure. By using confocal microscopy to examine the incorporation of fluorescently labeled proteins, spatial control over protein localization was exhibited. By controlling the loading quantity and localization of the model protein through the mineral thickness, a desired release profile can be achieved. A desired and effective delivery system of biological agents utilizing coprecipitation for bone regeneration can therefore be designed.

Keywords: Coprecipitation; Biomineralization; Biomimetic coating; Protein localization; Simulated body fluid (SBF); Hydroxyapatite-drug

1. Introduction

An ideal bone tissue engineering approach would incorporate osteoconductivity and osteoinductivity into the design of the supporting biomaterial, as well as biocompatibility, degradability, mechanical integrity, and the ability to support cell transplantation. Direct bonding between an implant and bone, the ultimate goal of osteoconductivity, may occur if a layer of bone-like mineral forms on the surface of the implant [1]. It has therefore been hypothesized that formation of a bone-like mineral layer within the pores of a tissue engineering scaffold may enhance the conduction of host cells into scaffolds [2], and also enhance osteogenic differentiation of transplanted cells seeded on scaffolds [3]. Such a biomimetic system maintains porosity, which is important to cell migration, as well as biocompatibility, mechanical integrity, and degradability [1,2]. Such composite scaffolds can also serve as reservoirs for growth factors [4]. While the polymer component serves as a carrier for the growth factor, the bone-like mineral component enhances the osteoconductivity and mechanical properties of the scaffold, allowing the composite to serve as a platform for the three tissue engineering approaches of conduction, induction and cell therapy.

*Corresponding author. Tel.: +1 734 764 2206; fax: +1 734 647 2110.
E-mail address: dhkohn@umich.edu (D.H. Kohn).

0142-9612/$ - see front matter © 2005 Elsevier Ltd. All rights reserved.
doi:10.1016/j.biomaterials.2005.07.043

Osteoinductive properties can be integrated into a scaffold using methods to immobilize proteins to surfaces such as adsorption, cross-linking, covalent binding, and entrapment, each of which results in different loading efficiencies and levels of protein retention [5]. Growth factors have been adsorbed to calcium phosphate ceramic surfaces, allowing these materials to serve as delivery systems [6,7]. Variations of protein adsorption onto bioceramics include dispersing a growth factor over the surface of porous hydroxyapatite [8,9], adsorbing antibiotic to each new layer of mineral deposited [10], and binding ceramic pellets together with gel with the growth factor adsorbed to the surface of the pellets [11]. These techniques are dependent on two factors: the substrate, and the specific growth factor used. The release profile of a surface adsorbed growth factor is rapid release, followed by a slower release based on the chemical and/or physical attraction between the material and the growth factor [12,13]. In some cases, however, a more sustained release or a pulsatile release is required for a growth factor to be effective.

Coprecipitation of proteins and calcium phosphate is another method that has been used to incorporate growth factors on metal substrates, such as titanium alloy implants [14–16]. An important advantage to this approach is the ability to produce calcium phosphate coatings at a physiological temperature, therefore minimizing conditions that would change the biological activity of the factors [17,18]. Coprecipitation leads to a more controlled protein release in comparison to adsorption methods, as well as increases the protein loading capacity [14]. Coprecipitation of bovine serum albumin, tobramycin, or recombinant human bone morphogenetic protein 2 and calcium phosphate onto titanium resulted in the retention of biological activity [14,15,19]. The main disadvantage of this system is the thickness of the coating created, which can be as thick as 50 μm [14]. If porous scaffolds were used as the platform for tissue engineering and growth factor release, the thick coatings could obscure the pores, restricting transport and cellular access, and possibly access to the growth factor.

In this study, we examined coprecipitation and surface adsorption schemes with respect to their abilities to control the spatial quantity and localization of a model protein, bovine serum albumin (BSA), that is incorporated into a biomimetic apatite layer nucleated onto polylactic-*co*-glycolic acid (PLGA) films. Protein incorporation was characterized by determining: (1) its presence in the film; (2) the quantity of protein incorporated; (3) the effects of rinsing on protein retention; (4) the morphology of the mineral with protein incorporated; and (5) the localization of the protein.

2. Materials and methods

2.1. PLGA film preparation

The films (approximately 30–80 μm thick) were prepared using 5 wt% PLGA, 85:15 PLA:PGA ratio (Alkermes), in chloroform solution. The films were cast in 10 cm glass Petri dishes, then covered with aluminum foil and air-dried for at least 24 h under a fume hood. The films were cut into $2 \times 2\,cm^2$ squares and etched in 0.5 M NaOH for seven minutes per side. They were rinsed with Millipore water before use.

2.2. Modified simulated body fluid and proteins used

A modified simulated body fluid (mSBF, which contains $2\times$ the concentration of Ca^{2+} and HPO_4^{2-} as standard SBF) was used to mineralize the films [20]. mSBF consists of the dissolution of the following reagents in Millipore water: 141 mM NaCl, 4.0 mM KCl, 0.5 mM $MgSO_4$, 1.0 mM $MgCl_2$, 4.2 mM $NaHCO_3$, 5.0 mM $CaCl_2 \cdot 2H_2O$, and 2.0 mM KH_2PO_4, whereas standard SBF contains 2.5 mM $CaCl_2 \cdot 2H_2O$, and 1.0 mM KH_2PO_4. mSBF was prepared at 25 °C and titrated to pH 6.8 using NaOH to avoid homogeneous precipitation of calcium phosphate. BSA was obtained from Sigma-Aldrich (A3294). Fluorescein-isothiocyanate (FITC)-labeled BSA was used in the protein localization experiments (Sigma-Aldrich, A9771).

2.3. Protein incorporation methods

In order to compare coprecipitation versus adsorption and quantities of protein loaded via the different protein incorporation methods, the following groups were examined: (1) 6 days coprecipitation of apatite and BSA; (2) 3 days apatite mineralization, 3 days BSA adsorption; (3) 3 days apatite mineralization, 3 days coprecipitation of apatite and BSA; (4) 3 days apatite mineralization, 2 days BSA adsorption, 1 day apatite mineralization; (5) 3 days apatite mineralization, 2 days coprecipitation of apatite and BSA, 1 day apatite mineralization; (6) 3 days apatite mineralization, 3 days acid etched BSA adsorption (10 mM EDTA); and (Control) 6 days apatite mineralization.

For mineralization, films were submerged in 40 ml of mSBF. Coprecipitation was accomplished by submerging the films in 40 ml of mSBF containing 200 μg/ml of BSA. Both mineralization and coprecipitation were carried out at 37 °C and the solutions were exchanged daily in order to replenish the ion concentration to supersaturated levels. For the samples subjected to adsorption, 0.25 ml of phosphate buffered saline (PBS) containing 200 μg/ml BSA was pipetted onto each film per day of adsorption. For Group 6, the protein was adsorbed to the surface using 10 mM ethylenediaminetetraacetic acid (EDTA), a technique which is based on higher protein retention to etched surfaces [9].

2.4. Protein presence

The incorporation of BSA was determined using Fourier Transform Infrared Spectroscopy (Spectrum BX FT-IR, Perkin-Elmer). The calcium phosphate coatings were scraped

off each of the samples ($n = 2$) using a ratio of approximately 300:1 of KBr to sample coating. A pellet was then prepared from this mixture. FT-IR spectra were recorded from 400 to 4000 cm^{-1} and baseline corrected.

2.5. Protein quantification

BSA was quantified using a Micro-Bicinchoninic acid (BCA) assay or BCA assay (Pierce, IL), depending on the concentration range. Samples ($n = 7$) were demineralized in 10 mM HCl. The samples were placed on a magnetic stir plate and agitated at 300 rpm for three days. The samples were incubated in reagents containing Na_2CO_3, $NaHCO_3$, bicinchoninic acid, $Na_2C_4H_4O_6 \cdot 2H_2O$ in 0.1 M NaOH, and 4% cupric sulfate pentahydrate, provided in the kit at 60 °C for one hour for the Micro-BCA assay, or for half hour for the BCA assay. Absorbance was measured using a UV spectrophotometer (SmartSpec 3000, BioRad) at 562 nm, and BSA concentration was determined based on standards. The BSA concentration in each of the groups was normalized to mineralized control concentrations.

2.6. Protein retention

To remove excess protein, samples were rinsed by gently dipping each film ($n = 7$) in Millipore water for 10 s. Samples were dried in a fume hood and placed in a vacuum desiccator until analyses were performed. Protein presence was confirmed using FT-IR, and protein concentration was quantified using the BCA assay kits.

2.7. Mineral and mineral/protein coating morphology

Mineral morphology with and without BSA was examined using scanning electron microscopy (Philips XL30 FEG Scanning Electron Microscope). Sample films ($n = 2$) were coated with a thin layer of gold and examined at 3 kV.

High-resolution transmission electron microscopy (HRTEM, Jeol 2010) was operated at an acceleration voltage of 200 kV to examine the crystal orientation of the mineral deposited on the polymer substrate. Rectangular glass plates, $2 \times 2\,cm^2$ and 1 mm thick were coated with PLGA and used as a substrate for apatite deposition. Samples with BSA incorporated via coprecipitation and samples without BSA incorporated were examined. Samples with BSA incorporation were coprecipitated for 7–8 days and samples without BSA were mineralized for 7–8 days. Additional days of coprecipitation or mineralization were needed in order to produce flakes that were appropriate for analyses. Calcium phosphate flakes were removed by breaking or dissolving PLGA between the calcium phosphate and the glass plate. The flakes were placed over a 1 mm diameter hole on a Cu grid. The grids were ion-milled on a liquid nitrogen stage at 5 kV using an incidence angle of 11–12°. Ion-milling was performed below −100 °C in order to prevent damage to the sample [21]. The specimen rotation drive rod was submerged in liquid nitrogen for at least 1 h prior to ion milling. To obtain a large but thin area on the mineralized film, a laser terminator was used to terminate power.

2.8. Protein localization

To visualize the spatial distribution of BSA in the different sample groups, a ratio of 7:1 of BSA:FITC-labeled BSA was used. Protein incorporation groups 1, 2, 3, 5, and the control group were studied ($n = 3$/group). Samples were produced by coating the surface of $2 \times 2\,cm^2$ glass cover slips with 5 wt% PLGA, 85:15 PLA:PGA ratio. The cover slips were dried in a fume hood and protein was incorporated as previously stated. After the incubation period, the samples were rinsed in three washes of Millipore water and dried in a fume hood. A small section was cut from the film and placed on a cover slide. A cover slip was glued on top of the sample and then the slide was viewed using confocal microscopy (Nikon TE 3000 Inverted Microscope) at an excitation wavelength of 488 nm. Using the BioRad Radiance 2000 LaserSharp imaging program, a series of images was taken in 2 μm intervals through the thickness of the film (approximately 100 μm) using 60× magnification oil immersion. A side depth profile through the thickness of the mineral layer on each of the films was obtained by stacking the series of images.

2.9. Statistical analysis

BCA assay results were analyzed with significance defined as $p < 0.05$. The Kruskal–Wallis One Way ANOVA on Ranks was used to analyze the effects of protein incorporation method on the amount of BSA within the mineral. The Student–Newman–Keuls post hoc comparison test was used for pair-wise comparisons. To determine the effects of rinsing, unrinsed and rinsed samples from each experimental group were analyzed via *t*-tests.

3. Results

3.1. Coprecipitation incorporated protein into the biomimetic mineral coating

The FT-IR spectra of all of the biomimetic mineral coatings show phosphate absorption bands of hydroxyapatite at ca. 1031, 600, and 561 cm^{-1}, and a carbonate peak at 1456 cm^{-1} (Fig. 1) [22]. An amide peak is shown for all three coprecipitated groups at 1652 cm^{-1} (Fig. 1) [23]. An additional smaller amide peak was also detected at 1539 cm^{-1} [23]. A peak at ca. 1635 cm^{-1}, near one of the amide peaks, is apparent in the mineralized control as well as the surface adsorbed samples, and is associated with the presence of water or octacalcium phosphate [22].

3.2. Coprecipitation resulted in significantly higher incorporation

The different protein incorporation methods resulted in significantly different amounts loaded into the films, $p < 0.001$ (Fig. 2). The results are provided as the concentration (μg/ml) of protein in 10 mM HCl

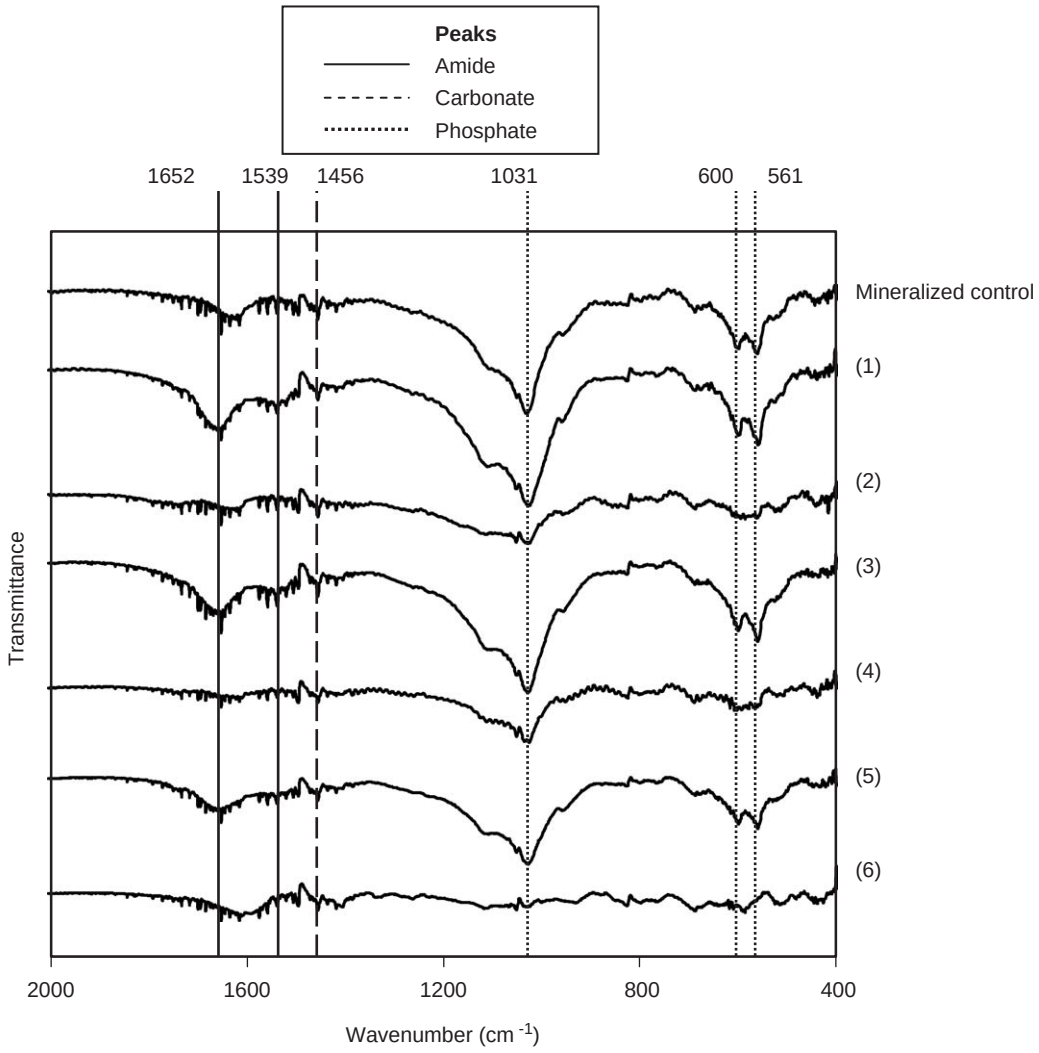

Fig. 1. Representative FT-IR spectra for the mineral-protein samples formulated via each of the following techniques: mineralized control, (1) 6 day coprecipitation, (2) 3 day mineralization, 3 day adsorption, (3) 3 day mineralization, 3 day coprecipitation, (4) 3 day mineralization, 2 day adsorption, 1 day mineralization, (5) 3 day mineralization, 2 day coprecipitation, 1 day mineralization, and (6) 3 day mineralization, 3 day acid etched adsorption. The phosphate (1031, 600, 561 cm^{-1}) peaks are denoted by dotted lines, a carbonate (1456 cm^{-1}) peak is denoted by a dashed line, and the amide (1652 and 1539 cm^{-1}) peaks are denoted by solid lines. Amide peaks are shown for all three coprecipitation groups.

(demineralization solution). All three coprecipitation groups (1, 3, 5) have significantly higher amounts of protein ($p<0.05$) in comparison to the three surface adsorption groups (2, 4, 6) (Fig. 2). When comparing the coprecipitation groups, protein loading was also significantly higher for Group 3 (3 day mineralization, 3 day coprecipitation) compared to Group 1 (6 day coprecipitation), and Group 5 (3 day mineralization, 2 day coprecipitation, 1 day mineralization), $p<0.05$. When comparing the surface adsorption groups, protein loading was significantly less for Group 4 (3 day mineralization, 2 day surface adsorption, 1 day mineralization) compared to Group 2 (3 day mineralization, 3 day surface adsorption) and Group 6 (3 day mineralization, 3 day surface adsorption using acid), $p<0.05$.

3.3. Coprecipitation leads to higher protein retention in comparison to adsorption

After rinsing to remove excess protein from the surface, amide peaks were still apparent in the spectra of the coprecipitated samples (Fig. 3). The amide (1652 and 1539 cm^{-1}), carbonate (1456 cm^{-1}), and phosphate (1031, 600, and 561 cm^{-1}) peaks that were present in the unrinsed samples were also denoted in spectra of most of the coprecipitation rinsed samples. The amide peak intensity decreased for Group 3 (3 day mineralization, 3 day coprecipitation), and for Group 5 (3 day mineralization, 2 day coprecipitation, 1 day mineralization) after rinsing (e.g. compare the peak at 1652 cm^{-1} in Fig. 3 to Fig. 1).

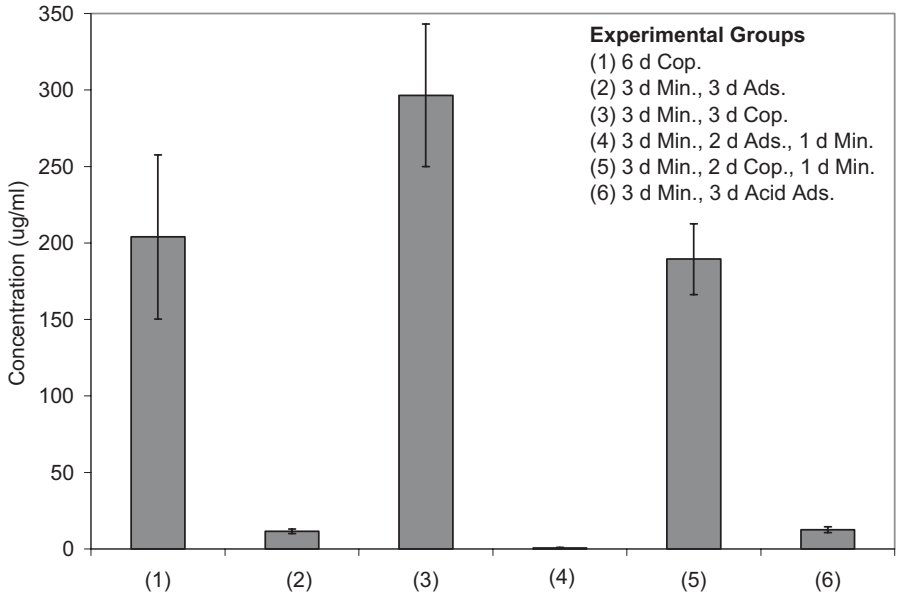

Groups	6 d Cop.	3 d Min., 3 d Ads.	3 d Min., 3 d Cop.	3 d Min., 2 d Ads., 1 d Min.	3 d Min., 2 d Cop., 1 d Min.	3 d Min., 3 d Acid
6 d Cop.						
3 d Min., 3 d Ads.						
3 d Min., 3 d Cop.						
3 d Min., 2 d Ads., 1 d Min.						
3 d Min., 2 d Cop., 1 d Min.						
3 d Min., 3 d Acid						

Fig. 2. Protein quantification for the mineral-protein samples via the following methods of protein incorporation: (1) 6 day coprecipitation, (2) 3 day mineralization, 3 day adsorption, (3) 3 day mineralization, 3 day coprecipitation, (4) 3 day mineralization, 2 day adsorption, 1 day mineralization, (5) 3 day mineralization, 2 day coprecipitation, 1 day mineralization, and (6) 3 day mineralization, 3 day acid etched adsorption. The results are provided as a protein concentration (μg/ml) in 10 mM HCl. Different incorporation methods resulted in significantly different amounts of protein loaded into the films, $p<0.001$. In the table, pair-wise comparisons of each of the groups were performed using the Student–Newman–Keuls post hoc test, significance is $p<0.05$ for the gray boxes. The white boxes show no significant difference between the two groups compared. The coprecipitation groups had a significantly higher quantity of protein loaded into the mineralized films in comparison to the surface adsorption groups.

While rinsing significantly affects protein retention in the surface adsorbed samples, there was no significant difference in retention when the coprecipitated samples were rinsed (Table 1). The efficiency of protein retention of each group was determined by obtaining the ratios of the quantity loaded after rinsing to the quantity loaded before rinsing. A ratio of approximately 1 is indicative of high protein retention after rinsing. A ratio much less than 1 is indicative of low protein retention. Two surface adsorption groups (Groups 2 and 6) showed significantly lower protein loaded onto the films after rinsing ($p<0.001$). The one exception was Group 4 (3 day mineralization, 2 day surface adsorption, 1 day mineralization), $p = 0.126$.

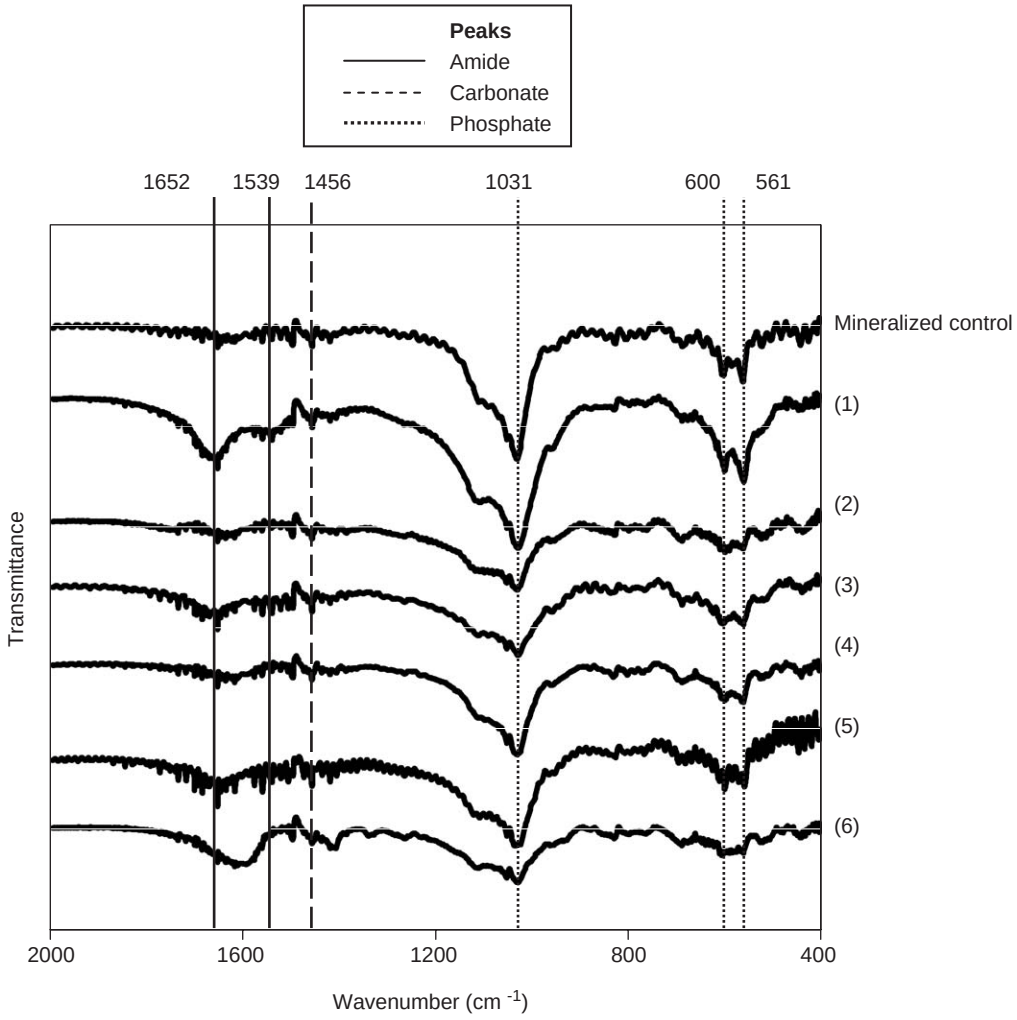

Fig. 3. Representative FT-IR spectra after rinsing for the mineral-protein samples formulated via each of the following techniques: mineralized control, (1) 6 day coprecipitation, (2) 3 day mineralization, 3 day adsorption, (3) 3 day mineralization, 3 day coprecipitation, (4) 3 day mineralization, 2 day adsorption, 1 day mineralization, (5) 3 day mineralization, 2 day coprecipitation, 1 day mineralization, and (6) 3 day mineralization, 3 day acid etched adsorption. The phosphate (1031, 600, 561 cm^{-1}) peaks are denoted by dotted lines, a carbonate (1456 cm^{-1}) peak is denoted by a dashed line, and the amide (1652 and 1539 cm^{-1}) peaks are denoted by solid lines. The amide peak at 1652 cm^{-1} decreased for Groups 3 and 5 following rinsing.

Table 1
Protein retention after rinsing

Groups	Ratio (rinsed/unrinsed)	St. dev. of ratios	Significance
(1) 6 d Cop.	1.23	0.43	0.148
(2) 3 d Min., 3 d Ads.	0.22	0.09	<0.001
(3) 3 d Min., 3 d Cop.	0.97	0.17	0.597
(4) 3 d Min., 2 d Ads., 1 d Min.	0.66	0.47	0.126
(5) 3 d Min., 2 d Cop., 1 d Min.	1.10	0.16	0.119
(6) 3 d Min., 3 d Acid Ads.	0.38	0.12	<0.001

Ratios of the amount of protein incorporated in the rinsed to unrinsed samples were calculated. Significant differences between the rinsed and unrinsed samples were determined using *t*-tests. All coprecipitation groups showed no significant difference between unrinsed and rinsed samples while the surface adsorption groups showed a more significant difference ($p<0.001$) from unrinsed to rinsed samples for two groups.

3.4. Protein coprecipitation changed mineral morphology

Incorporation of BSA via coprecipitation led to changes in the plate-like mineral morphology observed in mineralized controls, while BSA incorporation via surface adsorption did not change the plate-like mineral (Fig. 4). Control samples (6 day mineralization) exhibited plate-like morphology that is well defined with sharp edges (Fig. 4, control). Differences in morphology were found between the surface adsorbed and the coprecipitated samples. For the 6 day coprecipitation (Panel 1) and the 3 day mineralization, 3 day coprecipitation samples (Panel 3), the crystal plates were more rounded and there was less growth out of plane of the substrate due to the incorporation of BSA into the mineral. For the 3 day mineralization, 3 day

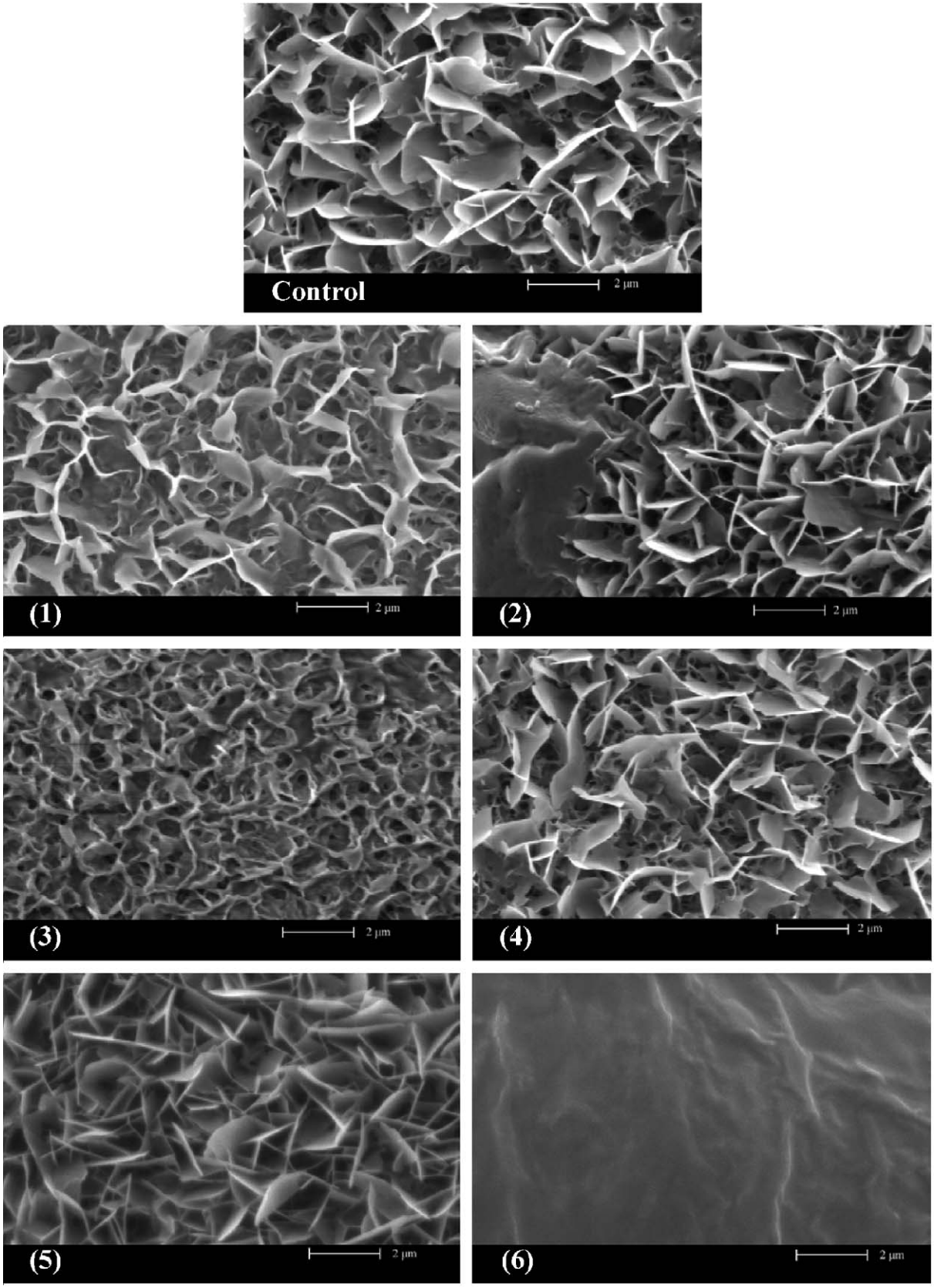

Fig. 4. SEM images of representative samples examined from each of the following groups (magnification 10,000 ×): (Control) 6 Day mineralization, (1) 6 day coprecipitation, (2) 3 day mineralization, 3 day adsorption, (3) 3 day mineralization, 3 day coprecipitation, (4) 3 day mineralization, 2 day adsorption, 1 day mineralization, (5) 3 day mineralization, 2 day coprecipitation, 1 day mineralization, and (6) 3 day mineralization, 3 day acid etched adsorption. BSA incorporation via coprecipitation leads to changes in the plate-like mineral structure that is observed in the control, while BSA adsorption does not change the mineral morphology.

coprecipitation samples (Panel 3), changes were apparent due to the absence of definable sharp plate edges. The 3 day mineralization, 2 day coprecipitation, 1 day mineralization sample (Panel 5), where the last day of treatment was mineralization without protein addition, showed similar plate-like structures to the control. The presence of the pipetted PBS/BSA solution on the mineral surface in the 3 day mineralization, 3 day adsorbed sample is characterized by the smooth material that appears on the left hand side of the image (Panel 2). Although the presence of PBS/BSA was not as apparent in the 3 day mineralization, 2 day surface adsorption, 1 day mineralization sample (Panel 4), the plate-like structures were similar to the control. The plate-like structures were not rounded like the structures that were present in the 6 day coprecipitation sample (Panel 1) or in the 3 day mineralization, 3 day coprecipitation samples (Panel 3). The acid etched sample (Panel 6) shows complete coverage of the acid/protein over the entire surface of each nucleation site resulting in smooth coverage.

HRTEM images of the films (A) without and (B) with BSA coprecipitation displayed plate-like apatite (Fig. 5). The size, shape, and distribution of the apatite crystals did not appear to be affected by the presence of BSA. However, a careful examination of the samples revealed that the coprecipitated apatite consisted of locally parallel layers, all parallel to the long axis of the plates (Fig. 5B, marked with arrows) whereas the layers were not visible in the samples without BSA coprecipitation (e.g. Fig. 5A). Diffraction patterns from the samples (A) without and (B) with BSA coprecipitation exhibited differences in the crystallographic orientations. The (002) ring observed in the samples without BSA (A) is not visible in the BSA coprecipitated samples (B).

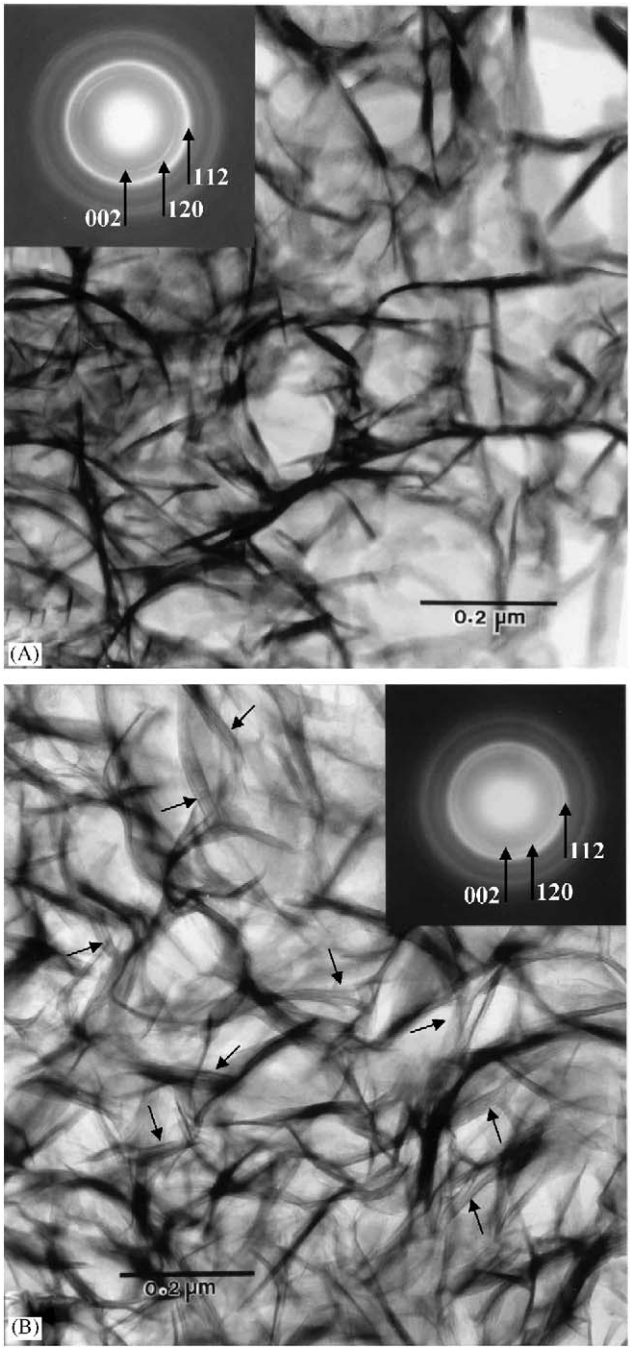

Fig. 5. Transmission electron microscope images of the mineral crystals: (A) mineralized sample without BSA and diffraction pattern showing the presence of the (002) ring, (B) mineralized sample with BSA via coprecipitation and diffraction pattern showing the absence of the (002) ring. Arrows in (B) mark apatite that consists of locally parallel layers, all parallel to the long axis of the plates. Arrows in the diffraction patterns of (A) and (B) mark the diffraction rings. The size, shape, and distribution of the crystals do not appear to be affected by the presence of the protein; however, there are differences exhibited in the orientation of the crystals.

3.5. *Coprecipitation allows for control over the localization of the protein*

For the 6 day coprecipitation sample (Group 1), fluorescence was present throughout the thickness of the mineral layer (Fig. 6, Panel 1). At the bottom of the mineral layer (layer closest to the polymer substrate), fluorescence occurred in the center of each nucleation site, and increased in intensity as more mineral and protein were deposited. In Group 2 (3 day mineralization, 3 day surface adsorption) little of the protein was adsorbed to the surface of the mineralization sites. Also, because the protein was surface adsorbed, the fluorescence was only on the surface of the mineral. Images closer to the polymer substrate show the fluorescence surrounding a dark circular center. Group 3 (3 day mineralization, 3 day coprecipitation) demonstrated a similar principle to Group 2. The images closest to the substrate show fluorescence surrounding a dark center; towards the top of the mineral layer, fluorescence was exhibited throughout the entire mineralization site. For Group 5 (3 day mineralization, 2 day coprecipitation, 1 day mineralization), fluorescence occurred as a shell

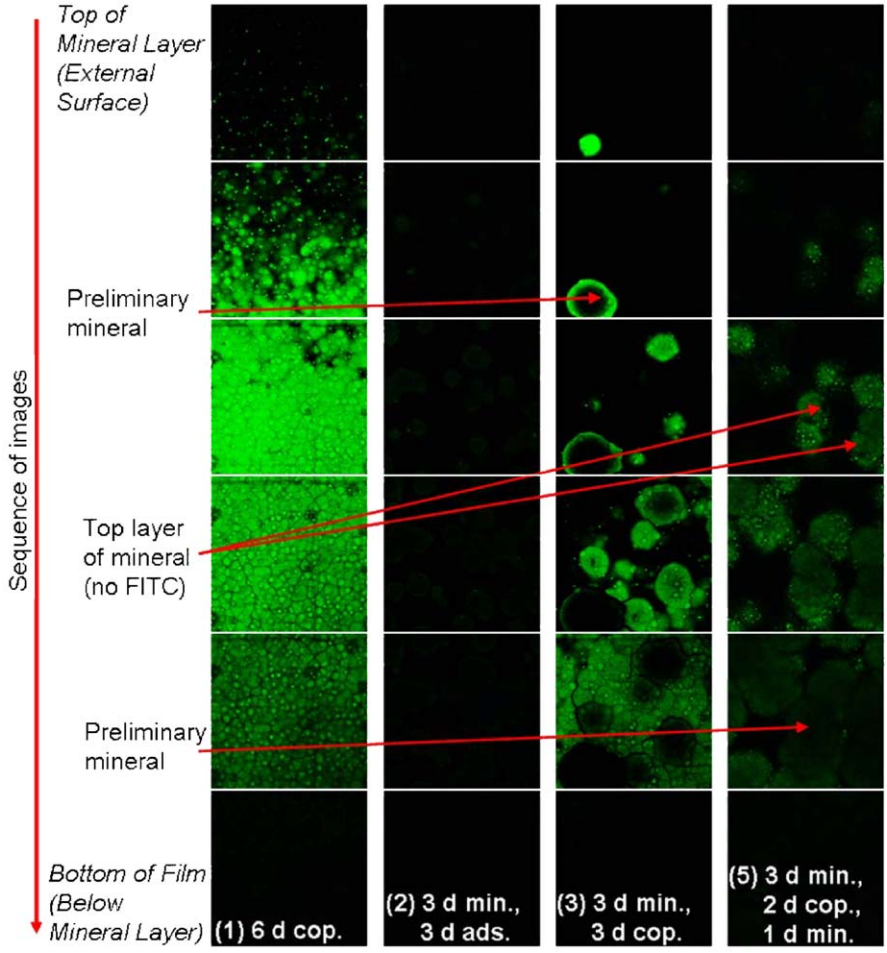

Fig. 6. Images through the thickness of the mineral layer containing FITC-labeled BSA taken using confocal microscopy. Spatial distribution of the protein through the thickness of the mineral layer is exhibited for the following incorporation techniques: (1) 6 day coprecipitation, (2) 3 day mineralization, 3 day adsorption, (3) 3 day mineralization, 3 day coprecipitation, and (5) 3 day mineralization, 2 day coprecipitation, 1 day mineralization. Fluorescence can be seen where coprecipitation or adsorption had occurred. The 6 day and 3 day coprecipitation groups were taken at the same gain and offset while the 3 day adsorption and 2 day coprecipitation groups were taken at a higher gain and offset in order to image the fluorescence. Control over the spatial distribution of the protein is shown by the presence of fluorescence through the thickness of the mineral for the different coprecipitation groups.

closer to the polymer substrate. At the surface of the mineral (top image), darker circles were also present and fluorescence was less intense. The additional dark circles were due to the additional day of mineralization that occurred for those samples. The mineralization that occurred on the last day had no protein incorporated; therefore fluorescence should not be present.

Side depth profiles, which were obtained by stacking the images acquired through the 100 μm thickness of mineral and substrate, show fluorescence through the thickness (Fig. 7). Consistent fluorescence occurred over a flat surface in the 6 day coprecipitation samples (Panel 1), which is not the case for the other groups. The 3 day mineralization, 3 day coprecipitation sample (Panel 3), and the 3 day mineralization, 2 day co-precipitation, 1 day mineralization sample (Panel 5) both showed an uneven fluorescence due to the mineral nucleation sites that occurred before FITC-labeled BSA was incorporated. In the 3 day mineralization, 3 day surface adsorption sample (Panel 2) fluorescence is also uneven, again due to the presence of the mineral nucleation sites that do not contain FITC-labeled BSA.

4. Discussion

There are various ways to immobilize proteins to surfaces, including physical adsorption, cross-linking, covalent binding, and entrapment. These methods have varying loading efficiency and varying levels of protein retention with manipulation [5]. Physical adsorption leads to low levels of loading while entrapment maintains high levels of loading; protein retention is low for physical adsorption and high for entrapment

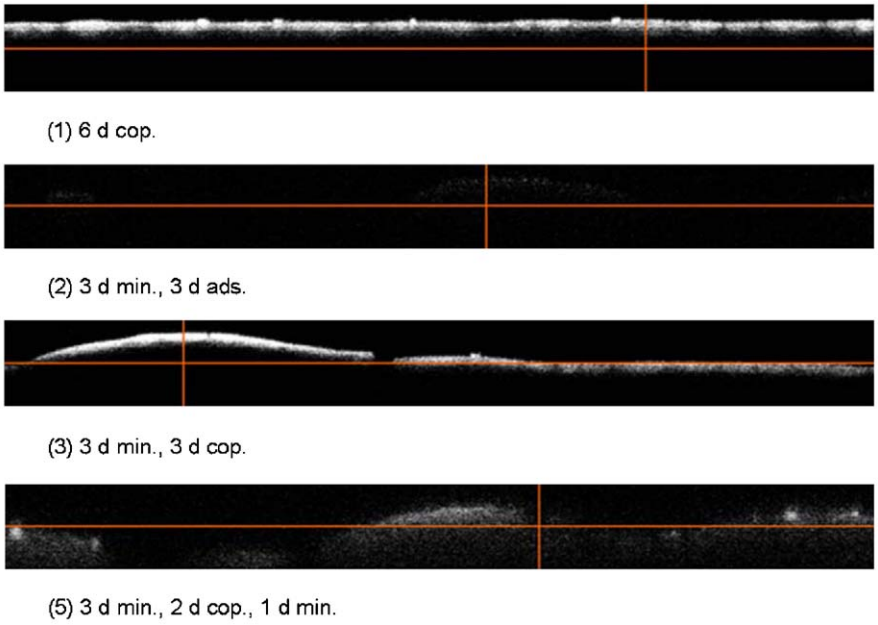

Fig. 7. Side depth profiles through the thickness of the mineral were obtained by stacking each series of images from Fig. 6, resulting in an image of the cross section of the film through the mineral layer and polymer substrate. The following groups were examined: (1) 6 day coprecipitation, (2) 3 day mineralization, 3 day adsorption, (3) 3 day mineralization, 3 day coprecipitation, and (5) 3 day mineralization, 2 day coprecipitation, 1 day mineralization. The side depth profiles show minimal protein incorporation for the adsorption group, whereas, all three of the coprecipitation groups show protein incorporation at varying locations through the thickness of the mineral.

techniques. While coprecipitation of mineral and protein has been investigated using titanium alloy implants and supersaturated calcium phosphate solutions, it has not been investigated on a polymer substrate. The focus of this study has been on the use of mSBF and BSA to form a thin organic/inorganic layer on an organic film at a physiological pH, temperature, and pressure, leading to spatially controlled protein localization within the mineral layer. Using BSA as the model protein, we have demonstrated that more protein can be incorporated into a mineral layer nucleated onto PLGA films via coprecipitation than via surface adsorption, and coprecipitation also allows for more control over protein localization in comparison to surface adsorption. By being able to control protein loading and spatial localization, it is hypothesized that a desired biological response can be elicited due to the resultant protein or growth factor release profile.

The presence of the amide bands in the FT-IR spectra showed that BSA was incorporated into both the coprecipitated and the surface adsorbed mineral, with a slight difference in amide intensity. The presence of phosphate and carbonate groups confirmed the presence of a carbonated apatite mineral [22].

Coprecipitation incorporates significantly more protein into a biomimetic apatite layer than surface adsorption. BSA is an acidic protein that is negatively charged at a pH of 6.8, therefore electrostatic interactions are important [24]. Through the interactions of its COOH groups, BSA binds to the Ca^{2+} on the surface of the mineral [24]. Another possibility is a conformational change upon attachment of BSA to the mineral surface, resulting in the exposure of NH_3^+ groups, and therefore interactions between BSA and mineral would occur with the phosphate groups [24]. These interactions lead to higher incorporation via coprecipitation because mineral and protein were deposited together through the thickness of the mineral layer, whereas in adsorption, these interactions were limited to the surface.

The significant increase in protein quantity when using 3 day mineralization, 3 day coprecipitation in comparison to a 6 day coprecipitation suggests that the preliminary mineral layer that was deposited increases the affinity of the protein, thus increasing its incorporation. BSA is a negatively charged protein, and PLGA is a hydrophobic polymer. The mineral layer is both positively and negatively charged, and with the presence of this layer the protein can better interact with the biomaterial surface. In the current study, once BSA has been incorporated onto the mineral surface, it increases the affinity for additional calcium phosphate deposition through its interactions with Ca^{2+}. The initial precipitated mineral serves to attract more BSA to the surface [25], resulting in a cyclical process. With the 6 day coprecipitation group, the preliminary mineral layer is absent, therefore protein cannot be deposited as easily due to the absence of Ca^{2+} molecules.

There was no significant difference in protein loaded between 6 day (Group 1) and 2 day (Group 5) coprecipitation. Thus, by premineralizing the films, fewer days of coprecipitation are needed to achieve the same amount of protein loaded. The significant decrease in protein amount between the 3 day mineralization, 2 day surface adsorption, 1 day mineralization group and the 3 day mineralization, 3 day adsorption group indicates that a polymer film that has protein adsorbed loses a majority of the protein once it is placed into solution due to weak surface interactions.

Coprecipitation resulted in significantly higher retention of protein following rinsing (Fig. 3 and Table 1). These data point to a stronger interaction of the protein with the mineral surface when coprecipitation is utilized. Higher protein retention is also the result of distributing the protein through the thickness of the apatite layer via coprecipitation, whereas in adsorption, the protein is bound to just the apatite surface. With surface adsorption, a large percentage of the protein is lost to solution once the sample is rinsed, suggesting that the BSA desorbs from the mineral layer and is distributed back into solution [24].

By coprecipitating protein into the mineral, the morphology of the mineral changed. BSA coats the surface of the mineral and alters the plate-like structures. BSA is chemically bound into or onto calcium phosphate, as indicated by the change in morphology and composition of the crystals in this study, as well as the absence of BSA release without the dissolution of calcium phosphate [17].

The addition of BSA, especially higher concentrations, results in a decrease in the crystallinity of the calcium phosphate precipitates [26]. Decreasing crystallinity of the calcium phosphate decreases protein release rates, which can contribute to better control of release kinetics [27]. The reason for the difference in the crystallographic orientation between the mineralized samples and the coprecipitated samples may be attributed to the interaction between BSA and crystallographic structure of apatite. With coprecipitation, protein may be incorporated into the three-dimensional crystal latticework [14]. A model was recently suggested regarding the interaction between aspartic acid and apatite crystals, which proposed that aspartic acid was enclosed inside a fourfold carbonate substituted apatite unit cell [28]. Based on the analysis of the HRTEM images and the diffraction patterns, BSA also has an influence on the crystal structure during the nucleation and growth of the mineral. Apatite growth can be influenced by the presence of protein because of the strong affinity between Ca^{2+} and protein. Since the spatial distribution of Ca^{2+} is orientation dependent, the preferential growth orientation can be modified by the presence of BSA.

With coprecipitation, the localization of the protein throughout the mineral layer can be controlled by changing the coprecipitation scheme. By using a 6 day coprecipitation process, the protein is incorporated throughout the mineral layer, whereas with adsorption the protein is only on the surface of the mineral (Figs. 6 and 7). In coprecipitation, the mineral is depositing with the protein, therefore the protein is being incorporated simultaneously with the mineral. The different coprecipitation schemes that were examined in this study show that the spatial localization of the protein can be controlled by controlling the start and extent of coprecipitation.

The control of protein localization could be manipulated to control the release kinetics of growth factors or other biomolecules. By changing the number of days of coprecipitation, or times at which protein is added to the mineralizing solution, the release kinetics of a growth factor can be varied. Multiple growth factors or plasmid DNA could also be incorporated into the bone-like mineral layer and/or the polymer substrate. Bone-like mineral will increase osteoconductivity and mechanical properties [2,3], while growth factors or plasmid DNA will increase inductivity. DNA [29] and other proteins [12,15] bind to apatite crystals through affinity binding. By controlling the loading quantity and localization of the protein through the mineral thickness, a desired release profile can be achieved. Protein release kinetics from coprecipitation samples differ in comparison to surface adsorbed samples. The burst release profile at early time points from adsorbed samples is minimized, suggesting that the protein has become an integral part of the mineral layer [14].

5. Conclusion

At standard temperature and pressure, coprecipitation processes were used to incorporate a model protein, BSA, into a biomimetic carbonated apatite mineral nucleated onto PLGA films. Coprecipitation of apatite and protein increased the quantity of protein incorporated into the apatite, in comparison to surface adsorption of protein following apatite deposition. This study also showed that coprecipitation allows for higher protein retention following rinsing, in comparison to adsorption. Furthermore, coprecipitation of protein along with apatite allowed for control over the localization of protein through the apatite thickness. The higher protein loading of this biomaterial system, and ability to spatially control the location of protein within the apatite, along with the provisions of osteoconductivity and osteoinductivity, by the mineral and protein, respectively, are important requirements for designing a desired protein release profile and effective delivery system of biological agents for bone regeneration.

Acknowledgements

This research is supported by NIH DE 015411 (DHK), DE 13380 (DHK), and the National Science Foundation Graduate Research Fellowship (LNL). The authors would like to thank the University of Michigan Electron Microbeam Analysis Laboratory for the use of their scanning electron microscope. The authors would also like to thank Sharon Segvich and Laura Darjatmoko for their aid in manuscript revision and helpful advice.

References

[1] Hench LL. Bioceramics—from Concept to Clinic. J Am Ceram Soc 1991;74:1487–510.
[2] Murphy WL, Kohn DH, Mooney DJ. Growth of continuous bonelike mineral within porous poly(lactide-*co*-glycolide) scaffolds in vitro. J Biomed Mater Res 2000;50:50–8.
[3] Kohn DH, Shin K, Hong SI, Jayasuriya AC, Leonova EV, Rossello RA, Krebsbach PH. Self-assembled mineral scaffolds as model systems for biomineralization and tissue engineering. In: Landis WJ, Sodek J, editors. Proceedings of the Eighth International Conference on the Chemistry and Biology of Mineralized Tissues. Toronto, Canada: University of Toronto Press; 2005.
[4] Murphy WL, Peters MC, Kohn DH, Mooney DJ. Sustained release of vascular endothelial growth factor from mineralized poly(lactide-*co*-glycolide) scaffolds for tissue engineering. Biomaterials 2000;21:2521–7.
[5] Hoffman AS. Biologically functional materials. In: Ratner BD, Hoffman AS, Schoen FJ, Lemons JE, editors. Biomaterials science: an introduction to materials in medicine. San Diego: Academic Press; 1996. p. 124–30.
[6] Ripamonti U, Ma S, Reddi AH. The critical role of geometry of porous hydroxyapatite delivery system in induction of bone by osteogenin, a bone morphogenetic protein. Matrix 1992;12:202–12.
[7] Ripamonti U, Yeates L, Vandenheever B. Initiation of heterotopic osteogenesis in primates after chromatographic adsorption of osteogenin, a bone morphogenetic protein, onto porous hydroxyapatite. Biochem Biophys Res Commun 1993;193:509–17.
[8] Sumner DR, Turner TM, Urban RM, Leven RM, Hawkins M, Nichols EH, McPherson JM, Galante JO. Locally delivered rhTGF-beta(2) enhances bone ingrowth and bone regeneration at local and remote sites of skeletal injury. J Orthopaed Res 2001;19:85–94.
[9] Arm DM, Tencer AF, Bain SD, Celino D. Effect of controlled release of platelet-derived growth factor from a porous hydroxyapatite implant on bone ingrowth. Biomaterials 1996;17:703–9.
[10] Campbell AA, Song L, Li XS, Nelson BJ, Bottoni C, Brooks DE, DeJong ES. Development, characterization, and anti-microbial efficacy of hydroxyapatite-chlorhexidine coatings produced by surface-induced mineralization. J Biomed Mater Res 2000;53:400–7.
[11] Alam MI, Asahina I, Ohmamiuda K, Takahashi K, Yokota S, Enomoto S. Evaluation of ceramics composed of different hydroxyapatite to tricalcium phosphate ratios as carriers for rhBMP-2. Biomaterials 2001;22:1643–51.
[12] Midy V, Rey C, Bres E, Dard M. Basic fibroblast growth factor adsorption and release properties of calcium phosphate. J Biomed Mater Res 1998;41:405–11.
[13] Ziegler J, Mayr-Wohlfart U, Kessler S, Breitig D, Gunther KP. Adsorption and release properties of growth factors from biodegradable implants. J Biomed Mater Res 2002;59:422–8.
[14] Liu YL, Layrolle P, de Bruijn J, van Blitterswijk C, de Groot K. Biomimetic coprecipitation of calcium phosphate and bovine serum albumin on titanium alloy. J Biomed Mater Res 2001;57:327–35.
[15] Stigter M, de Groot K, Layrolle P. Incorporation of tobramycin into biomimetic hydroxyapatite coating on titanium. Biomaterials 2002;23:4143–53.
[16] Liu Y, Hunziker EB, Randall NX, de Groot K, Layrolle P. Proteins incorporated into biomimetically prepared calcium phosphate coatings modulate their mechanical strength and dissolution rate. Biomaterials 2003;24:65–70.
[17] Wen HB, de Wijn JR, van Blitterswijk CA, de Groot K. Incorporation of bovine serum albumin in calcium phosphate coating on titanium. J Biomed Mater Res 1999;46:245–52.
[18] Wen HB, Wolke JG, de Wijn JR, Liu Q, Cui FZ, de Groot K. Fast precipitation of calcium phosphate layers on titanium induced by simple chemical treatments. Biomaterials 1997;18:1471–8.
[19] Liu YL, Hunziker EB, Layrolle P, de Bruijn JD, de Groot K. Bone morphogenetic protein 2 incorporated into biomimetic coatings retains its biological activity. Tissue Eng 2004;10:101–8.
[20] Murphy WL, Mooney DJ. Bioinspired growth of crystalline carbonate apatite on biodegradable polymer substrata. J Am Chem Soc 2002;124:1910–7.
[21] Lee KH, Hong SI. Interfacial and twin boundary structures of nanostructured Cu–Ag filamentary composites. J Mater Res 2003;18:2194–202.
[22] Koutsopoulos S. Synthesis and characterization of hydroxyapatite crystals: a review study on the analytical methods. J Biomed Mater Res 2002;62:600–12.
[23] Xie J, Riley C, Kumar M, Chittur K. FTIR/ATR study of protein adsorption and brushite transformation to hydroxyapatite. Biomaterials 2002;23:3609–16.
[24] Wassell DTH, Hall RC, Embery G. Adsorption of bovine serum-albumin onto hydroxyapatite. Biomaterials 1995;16:697–702.
[25] Marques P, Serro AP, Saramago BJ, Fernandes AC, Magalhaes MCF, Correia RN. Mineralisation of two phosphate ceramics in HBSS: role of albumin. Biomaterials 2003;24:451–60.
[26] Dorozhkin SV, Dorozhkina EI. The influence of bovine serum albumin on the crystallization of calcium phosphates from a revised simulated body fluid. Colloid Surfaces A 2003;215:191–9.
[27] Barroug A, Kuhn LT, Gerstenfeld LC, Glimcher MJ. Interactions of cisplatin with calcium phosphate nanoparticles: in vitro controlled adsorption and release. J Orthop Res 2004;22:703–8.
[28] Sarig S. Aspartic acid nucleates the apatite crystallites of bone: a hypothesis. Bone 2004;35:108–13.
[29] Okazaki M, Yoshida Y, Yamaguchi S, Kaneno M, Elliott JC. Affinity binding phenomena of DNA onto apatite crystals. Biomaterials 2001;22:2459–64.